Hindawi Publishing Corporation
Journal of Biomedicine and Biotechnology
Volume 2011, Article ID 578128, 11 pages
doi:10.1155/2011/578128

Research Article

The Construction of Chimeric T-Cell Receptor with Spacer Base of Modeling Study of VHH and MUC1 Interaction

Nazanin Pirooznia,[1] Sadegh Hasannia,[2,3] Majid Taghdir,[1] Fatemeh Rahbarizadeh,[4] and Morteza Eskandani[1]

[1] *Department of Biology, Faculty of Science, University of Guilan, Rasht, Iran*
[2] *Department of Biochemistry, Biological Science, Tarbiat Modares University, Tehran, Iran*
[3] *National Institute of Genetic Engineering and Biotechnology, Tehran, Iran*
[4] *Department of Medical Biotechnology, Tarbiat Modares University, Tehran, Iran*

Correspondence should be addressed to Sadegh Hasannia, hasannia@guilan.ac.ir

Received 19 March 2011; Revised 24 May 2011; Accepted 2 June 2011

Academic Editor: Ayman El-Kadi

Adaptive cell immunotherapy with the use of chimeric receptors leads to the best and most specific response against tumors. Chimeric receptors consist of a signaling fragment, extracellular spacer, costimulating domain, and an antibody. Antibodies cause immunogenicity; therefore, VHH is a good replacement for ScFv in chimeric receptors. Since peptide sequences have an influence on chimeric receptors, the effect of peptide domains on each other's conformation were investigated. CD3Zeta, CD28, VHH and CD8α, and FcgIIα are used as signaling moieties, costimulating domain, antibody, and spacers, respectively. To investigate the influence of the ligation of spacers on the conformational structure of VHH, models of VHH were constructed. Molecular dynamics simulation was run to study the influence of the presence of spacers on the conformational changes in the binding sites of VHH. Root mean square deviation and root mean square fluctuation of critical segments in the binding site showed no noticeable differences with those in the native VHH. Results from molecular docking revealed that the presence of spacer FcgIIα causes an increasing effect on VHH with MUC1 interaction. Each of the constructs was transformed into the Jurkat E6.1. Expression analysis and evaluation of their functions were examined. The results showed good expression and function.

1. Introduction

Adaptive cancer immunotherapy can cause stimulation of the immune system in different ways, thus leading to the prevention of cancerous cellular growth [1–3]. Regarding the important role of T cells in cellular immunity against tumors, various strategies have been applied to increase the performance and specific activation of T cells against tumors [4–7]. The aim of T-cell engineering is modification of chimeric T-cell receptors (chTCRs), in order to achieve high chimeric antigen receptor (CAR) expression. In one kind of chimeric receptor, independent of MHC for antigen recognition, a monoclonal antibody with high specificity for the target antigen was used. In this way, the resulting chimeric fragment had all the properties required to produce the best response against a tumor, such as: penetration into the tumor, cytokine secretion, cytotoxicity, and good specificity against cancerous antigens. The three main moieties of chTCR are the signaling domain, extracellular spacer domain, and the molecule attached to the antigen [8–10]. The importance of chTCR is that the specific antibody in its structure activates the immune system against target molecules on tumors. In other words, they cause tumor-specific immunity.

Therefore, the main property of chTCR is its killing/effector action against the target protein, independent of a monoclonal antibody against a specific tumor antigen. chTCRs are in fact artificial receptors in which an antibody recognizes the specific tumor antigen that is attached to a T-cell triggering domain.

In this study, the antibody part of the camelid VHH fragment together with CD3Zeta as the signaling domain and

CD8α and FcgIIα representing the spacers were used as different parts of the chimeric receptor. In Chimeric receptors, the heterogenous protein fragments are fused together; hence they can affect each other's function and structure. Because of the importance of the preservation of antibody activity, the selection of the type of spacer has an exceptional importance. Therefore, accuracy of results derived from the theoretical studies can have an enormous impact. For this purpose, two spacers were selected. In the theoretical phase of the study, their effects on antibody structure were studied, and with regard to both simulation parameters, different chimeric constructs were constructed. Two chimeric fragments carried by the PCZ (pcDNA3.1Hygro+ CD28Zeta) vector were then expressed in Jurkat cell lines, and the theoretical findings were subsequently compared with the experimental data. Comparative studies involved an evaluation of the interaction strength during the binding process of the proteins that have a significant importance in understanding the binding process, thus enhancing the ability of designing heterogenous proteins as chimeric receptor structures. Besides disulfide bonds, electrostatic forces are also responsible for protein recognition and binding, and as such have long-range effects on chimeric proteins' structure, function, and interaction with ligands, such as the peptide antigen fragments. Therefore, calculation of electrostatic potential and investigation of factors which affect these forces are of vital importance [11–15].

In previous work it was shown that the results from docking of MUC1 with different type of antibodies are in good agreement with the attained results from dynamic force spectroscopy (DFS); and these results present molecular docking simulation as a powerful method to prediction of binding sites in molecular recognition [16].

Due to the fact that spacer and ligand (antigen) binding involves hydrophobic forces as well as hydrogen bonds, both of which act in short range, structural rearrangement, and regulation of specific and correct binding can occur, thus leading to a new antibody and spacer structure. Therefore, the effect of protein sequences on the antibody during this binding process and, eventually, their functions are highly significant. Furthermore, the results of the theoretical studies must be monitored and evaluated in parallel with the experimental procedures, because increases in VHH affinity and the target peptide in the antigen are not objective, and after binding, effective signal transduction through the inserted spacer in the chimeric structure must occur. Therefore, in this study, the importance of spacer structure, as spacer domain, for better antibody domain exposure and its effect on VHH conformation with regard to interaction with MUC1 were investigated.

2. Materials and Methods

2.1. Homology Modeling. The homology study was performed using the MODELLER program version 9v2 [17]. The models were constructed on the basis of the camelid heavy-chain antibody (with PDB code: 1G6V) for VHH, the T-cell coreceptor, CD8α (with PDB code: 1AKJ) and the crystal structure of α-glucokinase for spacer1, the ERBB-2 receptor protein-tyrosine kinase (with PDB code: 1IIJ), and the membrane protein stannin (SNN) for spacer2.

2.2. Molecular Dynamics Simulation. MD simulation was performed using the AMBER9 program [18] at the Department of Biophysics, Tarbiat Modares University (TMU), Tehran, Iran. The Ptraj program was used to extract the information regarding conformational changes and structural mobility of the structures. In all of the calculations the protonated form of the ionizable amino acid in pH = 7 was used. In order to neutralize the surface charge, positive and negative ions were added. In case of VHH no ion was added, but for VHH-SP1 and VHH-SP2, three and one chloride ions (Cl^-) were added, respectively. In the calculations, the ff03 square force model was used [19], and for computing electrostatic forces, the Particle-Mesh Ewald (PME) method was applied [20]. In all simulations, the molecule was placed in a water environment with the TIP3P water model as solvent [21], with a minimum solvent shell thickness of 8 Å.

The simulations began with the 5000 iterations of the energy minimization using the Steepest Descent method. Simulations were performed for 100-ps under NVT (constant number of particles or moles, volume, and temperature) conditions, and the temperature increased from 200 K to 300 K. Then, the simulations were performed for another 100-ps under NPT (constant number of particles or moles, pressure, and temperature) conditions so that the system reached equilibration at constant pressure. (The criteria for equilibration of the system under NPT conditions included total energy and density). Simulations continued for 5-ns under NPT condition and a scale of 2-fs was considered. In all simulations, the SHAKE algorithm was used to fix hydrogen bond trembling with other atoms. Finally, every 0.4-ps one structure was saved (in each simulation, 5000 structures were saved for the study).

2.3. Molecular Docking. The calculations regarding the interaction between MUC1 and VHH structures, which were obtained by MD simulations, were performed using 3D-Dock program. The structure of MUC1 was obtained from the Protein Data Bank (PDB ID: 1SM3). Docked structures were constructed using FTDock program [22]. The surface thickness of VHH was considered as 1.3 Å, and the Rpscore program was used to score all known complexes. For each calculation, 100 complexes with the highest score were selected using the multiDock program. Finally, the complexes at the lowest energy levels were selected and compared with each other.

2.4. Construction of Modified Chimeric T-Cell Receptor (TCR). For insertion of the two spacer fragments, CD8α and FcgIIα, a vector carrying chTCR named pcDNA3.1Hygro+ zeta CD28 IgG3 VHH was used [23]. For obtaining DNA from the two spacer sequences, peripheral white blood cells (WBCs) were obtained using the Ficoll-Paque solution (Pharmacia, Sweden), and cells were centrifuged for 20 min at 900 g. Total RNA from the WBCs was isolated by the nucleospin RNA II kit (Macherey-Nagel Duren, Germany), and first strand

cDNA was synthesized with M-MULV reverse transcriptase (MBI, Fermentas, St. Leon-Rot, Germany). Amplification of the CD28 fragment was carried out by P1 (Table 1) primers using *pfu* DNA polymerase according to the following temperature and time profiles: 94°C denaturation for 2 min (1 cycle), 30 cycles each of denaturation at 94°C for 20 s, annealing at 61°C for 30 s, extension at 72°C for 1 min, and a final extension at 72°C for 10 min (1 cycle). FcgIIα amplification was carried out using the above-mentioned material and P2 primers (Table 1) according to the following temperature and time protocols: 94°C denaturation for 2 min (1 cycle), 30 cycles each of denaturation at 94°C for 20 s, annealing at 64.9°C for 30 s, extension at 72°C for 1 min, and a final extension at 72°C for 10 min (1 cycle).

The amplified CD28 and FcgIIα fragments were separated by electrophoresis and purified from the agarose gel using the QIA-quick Gel Extraction Kit (Qiagen, Hilden, Germany). The purified fragments were then sequenced by the automated method. In order to cut out the IgG3 spacer fragment from the original vector carrying the chimeric cassette and insert the new spacers, the vector was first digested with Not1 (Fermentas) and *Xho1* (Fermentas) enzymes to become linear, and following electrophoresis, the linearized fragment was purified using the aforementioned kit. The linearized fragments were then ligated separately with the two digested spacer products (CD28 and FcgIIα) using T4 DNA ligase (TaKaRa, Kyoto, Japan). Two resulting vectors carrying the different spacer fragments were sent for sequencing to evaluate ligation accuracy. The two constructed vectors, pcDNA3.1Hygro+ Zeta CD28 CD8α VHH and pcDNA3.1Hygro+ Zeta CD28 FcgIIα VHH carrying the chimeric receptors were designated and pZCCV and pZCFV, respectively.

2.5. Transfection of Constructs into Prokaryotic Host and Jurkat Cell Lines. After confirmation of cloning by sequencing, the two new vectors carrying the CD28 and FcgIIα spacers were used to transfect the prokaryotic host (TG1), and following manipulation of the transfected host its DNA was extracted by QIAprepMiniprep Kit (QIAGEN) according to the manufacturer's instructions. Jurkat cells were harvested at the exponential phase of growth and centrifuged for 10 min at 200 g. The cells were then resuspended in RPMI 1640 containing 5% fetal calf serum (FCS). Cell numbers were then counted, and the cells were recentrifuged for another 5 minutes at 200 g. The supernatant was removed, and the Jurkat cells were resuspended in hypoosmolar electroporation buffer (Eppendorf, Hamburg, Germany). The cell concentration was adjusted to 1×10^6 cells per mL. Plasmid DNA (final concentration of 10–20 μg/mL in distilled water) was added to the cells and mixed. Samples of the cell suspensions (400 μL) were transferred into electroporation cuvettes with a 2 mm gap width (Eppendorf). Electroporation conditions included one pulse at 240 V for 40 ms using the Eppendorf system. After the delivery of the pulse, the cell suspension was allowed to stand in the cuvette for 5–10 min at room temperature. Cells were then left to recover for 24 h in nonselective media, followed by the selection of transfected cells in 800 mg/mL of hygromycin (Sigma-Aldrich, USA). Selected cells were maintained in the above media containing the same concentration of hygromycin for 10 days.

2.6. Reverse Transcriptase PCR (RT-PCR). Total RNA was isolated from 1×10^6 receptor-grafted and nontransfected Jurkat cells using the NucleoSpin RNA II system (Macherey-Nagel GmbH & Co KG). cDNA was synthesized using M-MuLV as described above. CD28-zeta PCR was performed using primers P3 (Table 1). It should be noted that intact Jurkat cells do not express the CD28-zeta chimera. β-actin was used as an internal control using primers P4 (Table 1). The abovementioned PCR reactions were carried out according to the following temperature and time profiles: 94°C denaturation for 5 min (1 cycle), 30 cycles each of denaturation at 94°C for 20 s, annealing at 58°C for 30 s, extension at 72°C for 50 s, and a final extension at 72°C for 10 min (1 cycle).

2.7. Functional Assay of CAR-Grafted Jurkat Cells. Proliferation of CAR-grafted Jurkat cells upon incubation with MCF7 cells: transfected and nontransfected Jurkat cells (1×10^5 cells per well) were cocultivated in 6-well plates with MCF7 tumor cells that had reached 70% confluency. Nontransfected Jurkat cells and those transfected with the pCDNA3.1 Hygro+ vector were used as controls. Suspended cells were harvested after 24 h of incubation at 37°C, and the collected viable cells (receptor-grafted and control Jurkat cells) were then counted. Tests were performed in duplicate wells and transfected and nontransfected Jurkat cells were counted in duplicate using a Neubauer cell counting chamber (Neubauer, Germany).

2.8. Cytotoxicity Assay. The specific cytotoxicity of receptor-grafted and control Jurkat cells against cancerous cells was measured. In this assay, healthy MCF7 cells were counted in duplicate as mentioned above, and dead cells were excluded via staining with trypan blue.

2.9. Designing a Bioassay for Interleukin-2 Secretion. Activity of the secreted Interleukin-2 (IL-2) in supernatants of the abovementioned cocultures was assessed in a bioassay test. In this assay, the proliferation of the IL-2-dependent T-cell line CTLL2 in the presence of secreted IL-2 was analyzed. At different dilutions of the coculture samples, supernatant proliferation was assessed by the MTT Cell Viability Assay Kit (Biotium, Hayward, CA). The 3-[4,5-dimethylthiazol-2-yl]-2,5-diphenyl tetrazolium bromide (MTT) assay was performed in 96-well plates. The CTLL2 cell line (1×10^4 cells per well) was cultured in RPMI 1640 medium containing 15% (v/v) FCS (without IL-2) for 24 h. Supernatants harvested from the two receptor-grafted and control Jurkat cells cocultured with MCF7 cells were diluted 1 : 2, 1 : 4, and 1 : 9 with fresh RPMI 1640 medium containing 15% (v/v) FCS and were then added in duplicate to the CTLL2 cells and incubated at 37°C for 22 h. After incubation, 10 mL of the MTT reagent was added to the wells and incubated for 3 h at

Table 1: Names, properties, and target sequences of PCR primers.

Primer name	Sequences	Target name
P1	5′CACGCGGCCGCAGCAACTCCATCATGTACTTCAGCCACTTC3′ 5′AGATGTAGATCTGGAGGGCGAAGTCCAGCCCCCTCGTGTGCAC3′	CD8α
P2	5′CCTCACGCGGCCGCACTGTCCAAGTGCCCAGCATG3′ 5′TTTTGGCTCGAGCCTGCAGTAGATCAAGGCCAC3′	FcgIIα
P3	5′AGAGTGAAGTTCAGCAGGAGC3′ 5′TGCTCTAGATGGCTGTTAGCGAGG3′	CD28ζ
P4	5′AGTAGGCTTTGTGGTTGATG3′ 5′CTGTCAGGAAAGGAGAAATC3′	β-actin

37°C. At the end of incubation, the medium was removed, and 100 mL of DMSO (Dimethyl sulfoxide) was then added to each well to dissolve the formazan crystals by pipetting up and down several times. Absorbance of each well was measured on an ELISA plate reader at a wavelength of 540 nm to obtain sample signal.

3. Results

3.1. Theoretical Studies

3.1.1. Molecular Dynamics Simulation. The results from the theoretical study are presented in four sections: (1) Simulation stability; (2) Structural fluctuation; (3) Simulation of VHH and MUC1 interaction; (4) Influence of surface charge distribution on the interaction.

(1) *Simulation Stability.* Simulation stability is investigated in three different ways; (a) RMSD; (b) Total energy changes; (c) Temperature and density.

(a) *RMSD.* One of the most frequently used measures of assessing the stability of an MD simulation over the course of time is the RMSD between the first coordinate and the generated structures in the trajectory, as follows:

$$\mathrm{RMSD} = \sqrt{\frac{1}{N}\sum\left(r_i^{\mathrm{ref}} - r_i^{\mathrm{gen}}\right)}, \quad (1)$$

where r_i^{ref} and r_i^{gen} denote the Cartesian coordinates for atom i in the first and generated structures, respectively. Therefore, RMSD values for the main chain atoms of VHH, VHH with the CD8α spacer and VHH with the FcgIIα spacer during 3 ns of the total 5 ns simulation time relative to the experimental structure were calculated (Figure 1(a)). As revealed in Figure 1, simulation of three structures showed good stability and no significant deviation from the previous structures after 3 ns. We can be sure that the obtained structures from the simulation were optimal and that the different structural regions affected each other. Hence, in each simulation, structures reached their final conformations.

(b) *Total Energy Changes.* Total energy changes during 100 ps of simulation time at the equilibrium phase under NPT conditions were carried out for the certitude ofsimulation stability (Figure 1(b)). As illustrated in Figure 2, the system's total energy at the equilibrium phase under fixed pressure conditions after 20 ps for all simulations remains constant.

(c) *Temperature and Density.* The temperature for VHH, VHH with CD8α and VHH carrying FcgIIα was 300 K, and the densities for VHH, VHH with CD8α and VHH with FcgIIα were 1/03 gr/cm^3, 1/00 gr/cm^3, and 1/00 gr/cm^3, respectively, that ultimately became fixed and stable, representing further proof of simulation stability.

(2) *Structural Fluctuations.* Fluctuation of the interacted molecules, especially fluctuation of the sequence involved in the interaction, is of particular importance in the manner of interaction and protein function efficiency. In some structural regions, with the presence of each of the two spacer sequences, VHH structural fluctuations in the presence of the CD8α spacer differ significantly from that in the presence of the FcgIIα spacer (Figure 2). It should be mentioned that the structural properties of the native VHH are considered as reference properties, and all the investigated properties in the presence of each spacer sequence in this study are compared with the reference structure (Figure 2). Regarding the comparison of the structural fluctuations of native VHH with that of VHH carrying CD8α, as illustrated in Figure 2, the increase in fluctuations is in the amino acid regions 5–13, 29–32, 112–117 and a decrease in fluctuations in the amino acid regions 58–61, 105–110, as compared with the reference structure. But when comparing the VHH structure carrying the FcgIIα spacer with that of the reference, the increase in fluctuations is in the amino acid region 30–36 and a decrease in fluctuations is in the regions 59–75, 86–96.

(3) *Simulation of VHH and MUC1 Interaction.* For denotation and comparison of residues involved in interaction, docking was done between VHH structures, with different spacer, which are obtained from molecular dynamic simulation and target sequence in MUC1 (SAPDTRPAP) (Table 2).

In each simulation 100 complexes were made, and complexes with most negative binding energy, which represent the important interaction in complexes, were selected. The results from docking native VHH with MUC1 indicate that specific amino acids from VHH participate in interaction

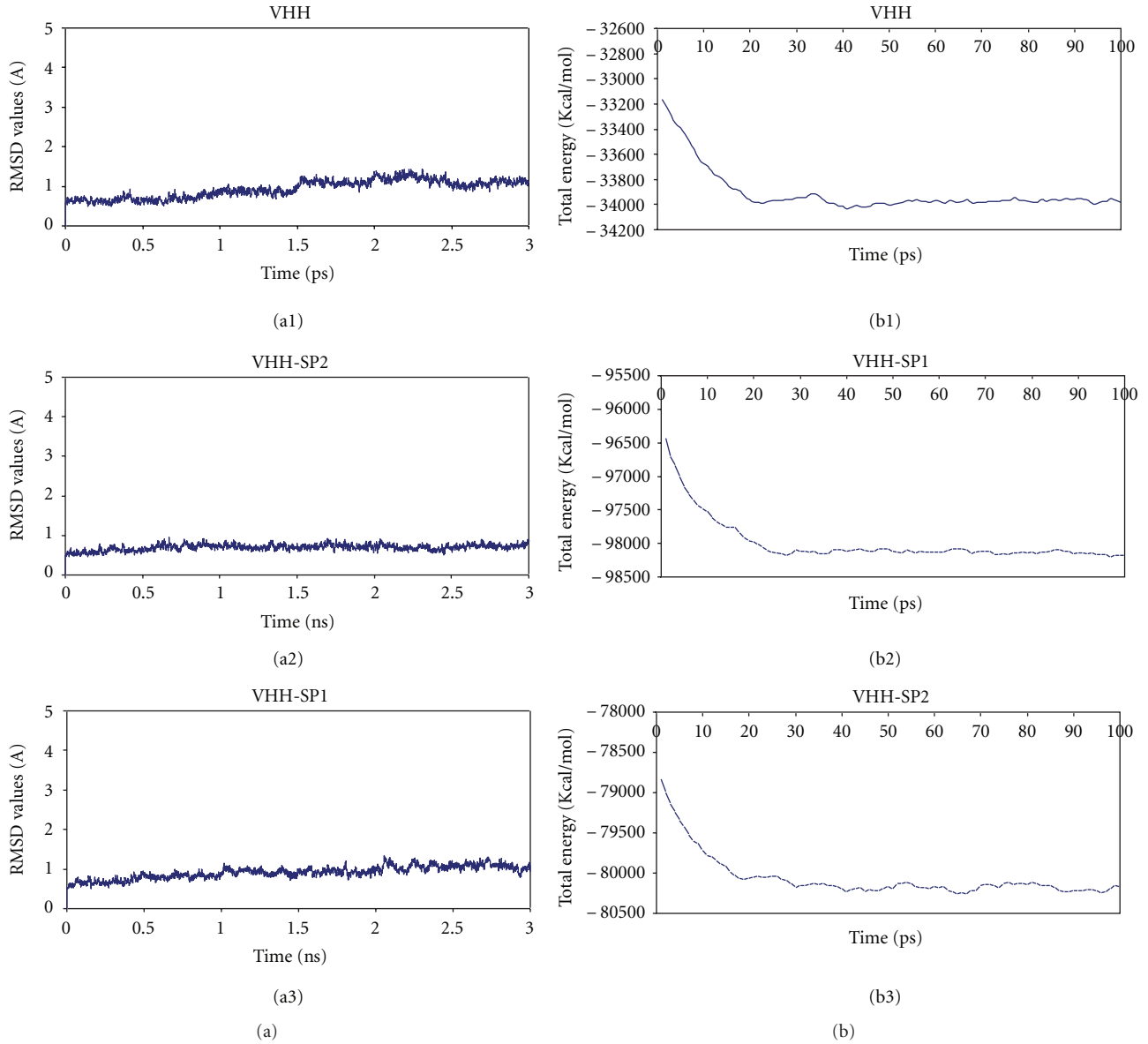

Figure 1: Comparison of RMSD and total energy values. RMSD values for the main chain atoms of (a1) VHH, (a2) VHH with CD8α spacer, and (a3) VHH with FcgIIα spacer during 3 ns of a total 5 ns simulation time. Total energy changes in 100 ps of simulation time for (b1) VHH, (b2) VHH with CD8α spacer, and (b3) VHH with FcgIIα spacer.

with target. In this simulation important regions involved in binding include amino acids 41–52, 108–117 with total binding energy −40.2 Kcal/mol. Docking VHH plus CD8α with MUC1 target sequence showed that regions 5–11, 113–121 take part in interaction, and total binding energy was −36.0 Kcal/mol. Docking results of VHH plus FcgIIα and MUC1 target sequence showed that amino acids 4–9, 102–105, 114–119 are involved and total binding energy was −46.9 Kcal/mol. Interaction simulation results in Table 2 revealed that C-terminal region of VHHs has a critical role in interacting with MUC1 target sequence. In interaction VHH-spacer FcgIIα with MUC1 N-terminal region of VHH and Arg103 are involved in binding and decrease total binding energy from −40.2 to −46.9 Kcal/mol. On the other hand Asp5 in MUC1 target sequence plays an important role in increasing of binding energy from −40.2 to −36.0 Kcal/mol.

(4) *Influence of Surface Charge Distribution on Interaction.* Since the most important factor in the orientation of macromolecules perior to interaction is long-range electrostatic forces, the molecule's surface charge distribution, which is the result of charged amino acids in the macromolecules has significant importance. In Figure 3, surface charge distribution of native VHH and VHH with each of the two spacers in interaction with the MUC1 target sequence (green color), especially the pattern of the charged amino acids' charge distribution in each simulated complex, is shown. It

Table 2: Binding energy of important residues involved in interaction between MUC1 with the different types of VHHs. (Units: Kcal/mol).

Involved residues in binding	VHH/MUC1			VHH-SP1/MUC1			VHH-SP2/MUC1		
	Total	VDW[a]	ELE[b]	Total	VDW	ELE	Total	VDW	ELE
VHH/VHH-sp1/sp2									
Glu5	0.0	0.0	0.0	−0.3	−0.1	−0.2	−6.4	−2.0	−4.4
Val6	0.0	0.0	0.0	−0.1	0.0	−0.1	−1.2	−1.2	0.0
Glu7	0.0	0.0	0.0	−6.2	−0.3	−5.9	−1.0	−0.3	−0.7
Gln9	0.0	0.0	0.0	−1.0	−0.8	−0.2	−0.2	0.0	−0.2
Gly48	−0.9	−0.9	0.0	0.0	0.0	0.0	0.0	0.0	0.0
Arg49	−4.2	−2.9	−1.3	0.0	0.0	0.0	0.0	0.0	0.0
Arg103	0.0	0.0	0.0	0.0	0.0	0.0	−2.2	−0.7	−1.5
Leu109	−2.0	−2.1	0.1	0.0	0.0	0.0	0.0	0.0	0.0
Gly110	−1.9	0.7	−2.6	0.0	0.0	0.0	0.0	0.0	0.0
Cys112	−1.6	−0.6	−1.0	0.0	0.0	0.0	0.0	0.0	0.0
Asp113	−1.5	−0.2	−1.3	−0.1	0.0	−0.1	0.0	0.0	0.0
Tyr114	−1.0	−0.7	−0.3	−0.5	−0.5	0.0	−2.7	−1.2	−1.5
Asn115	−2.2	−2.0	−0.2	−0.1	−0.4	0.3	−3.9	−1.6	−2.3
Tyr116	−0.7	−0.8	0.1	−2.7	−2.3	−0.4	−3.9	−2.8	−1.1
Trp117	−0.7	−0.7	0.0	−2.8	−1.9	−0.9	−0.6	−0.5	−0.1
Gln119	0.0	0.0	0.0	−1.1	−0.7	−0.4	0.0	0.0	0.0
MUC1									
Pro4	−1.4	−2.0	0.6	−0.3	0.0	−0.3	0.0	0.0	0.0
Asp5	−4.8	−2.6	−2.2	0.0	0.0	0.0	−7.7	−2.9	−4.8
Thr6	−1.0	−0.4	−0.6	−0.8	−0.7	−0.1	−0.3	−0.3	0.0
Arg7	−9.1	−4.2	−4.9	−9.3	−0.5	−8.8	−10.0	−0.7	−9.3
Pro8	−0.3	−0.4	0.1	−2.5	−2.5	0.0	0.0	0.0	0.0
Ala9	−0.5	−0.4	−0.1	−2.4	−2.4	0.0	−2.2	−2.1	−0.1
Pro10	−1.8	−1.8	0.0	−3.1	−2.5	−0.6	−3.2	−2.4	−0.8

[a] Van der Waals energy, [b] electrostatic energy.

must be noted that all figures are shown at a similar viewing angle. It can be concluded from Figures 3(c) and 3(d) that the VHH molecule is almost a dipole molecule, that is to say that the charge distribution in the molecule is not equal and the result is a negatively charged surface (red color) on one face of the molecule and a positively charged surface on the other face. The negatively charged surface is a suitable region for attracting the MUC1 target sequence, which has the arginine amino acid as the key amino acid. Figures 3(a), 3(b), and 3(c) also show little difference in the surface charge between the native VHH and VHH with each of the two spacers. This slight difference causes change in the orientation of the MUC1 target sequence during binding, thus leading to a distinction in binding energy. It should be noted that slight differences can significantly affect the binding half-life and effectiveness of the VHH interaction with the MUC1 target sequence.

3.2. Experimental Studies

3.2.1. Construction and Expression of pZCCV and pZCFV. Two Chimeric recombinant anti-MUC1 receptors with different spacers, CD8α and FcgIIα, which contain the anti-MUC1 nanobody were constructed. The two chimeric receptors contain transmembrane (CD28) and intracellular (CD3Zeta) moieties, which have been reported previously [23]. These constructs and the control (vector without the construct) were transformed into Jurkat cells. Expression of the transcript was evaluated by RT-PCR using P3 (for CD28Zeta amplification) and P4 (for β-actin, Table 1) primers (Figure 4).

3.3. Functional Assays

3.3.1. Increased Proliferation of CAR-Grafted Jurkat Cells upon Coculturing with MCF7 Cells. To monitor the changes in the growth rate of receptor-grafted Jurkat cells in the context of antigen simulation, MCF7 cells were co-cultured with transfected and nontransfected Jurkat cells. After 24 h, recombinant receptor-grafted Jurkat cell proliferation was substantially enhanced upon incubation with MCF7 tumor cells, while nontransfected Jurkat cells and pCDNA3.1Hygro+ transfected Jurkat cells had a significantly lower rate of proliferation in the presence of MCF7 tumor cells (Figure 5).

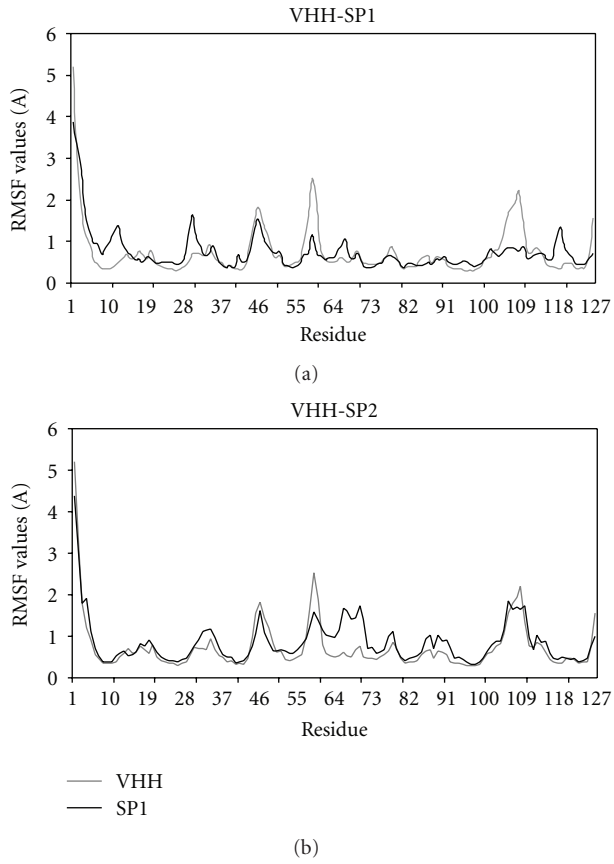

Figure 2: Comparison of structural fluctuation changes of native VHH with (a) VHH + CD8α, and (b) VHH + FcgIIα spacer.

3.4. Cytotoxicity Assay. CAR-grafted Jurkat cells were specifically activated, and the MCF7 cells were lysed with high efficiency, whereas no similar effect was observed in the nontransfected Jurkat cells and the control vector-transfected Jurkat cell culture (Figure 6).

3.5. Determination of Interleukin-2 Secretion. For the bioassay, CTLL2 cells were cultured in duplicate in the abovementioned coculture supernatants harvested from the receptor-grafted and nontransfected Jurkat cell dilutions. Figure 7 shows the higher proliferation rate of CTLL2 cells in the receptor-grafted Jurkat cell supernatant. Since the proliferation of CTLL2 is positively correlated to the IL-2 levels, these data indicate that receptor-grafted Jurkat cells produce more IL-2 in comparison with the nontransfected and the control vector-transfected Jurkat cells (Figure 7).

4. Discussion

T-cell production via genetic engineering of TCR is a new strategy for immunotherapy. In this method, α and β TCR genes are transferred to T cells against a specific antigen. Since this method does not need the separation of specific T cells, it is very functional and applicable. However, the use of this method has many problems too. TCR recognition process is MHC dependent. In severe phases of many cancers, MHC expression is reduced; however, T cells are available against cancer antigens, but they cannot recognize tumor cells. Many of the tumor antigens are glycolipids or carbohydrate antigens, and TCR cannot recognize these antigens [24, 25].

Another strategy makes use of antibody specificity to recognize cancer antigens, cytokine secretion, and killing of the cells by T lymphocytes. In this method, with the use of gene constructs containing chimeric T cells, they gain the ability to recognize different cancer antigens. In such gene constructs, antibody has the role of antigen recognition (in place of TCR), and the parts that are removed from lymphocyte have the role of signaling domain in T lymphocytes. Signals in the T lymphocyte finally lead to cytotoxic activity [26].

In this study, at first, two kinds of chimeric receptor genes constructed with a signaling domain and costimulating molecule were transferred to T-cell lymphocytes. It became clear that T lymphocytes, beside cytotoxic activity, have cytokine secretion capability, which can cause a second wave of stimulations and draw other immune system members to the tumor site. In subsequent investigations of this study, co-stimulating and signaling fragments were both placed in an individual gene construct which ultimately led to favorable results. Because this method takes advantage of antibody specificity, it is MHC independent, and thus this kind of treatment is unaffected by problems associated with low MHC levels [27].

Furthermore, the use of antibodies in gene constructs against different cancer antigens enables the application of chimeric receptors to many cancers. In fact, antibodies have the ability of recognizing glycolipid and carbohydrate antigens which are common in cancers. Of course chimeric receptors are not applicable to all cancers, but only to those in which surface antigens are reachable for antibody targeting [28].

Many of the accomplished studies have shown that the usage of chimeric receptors also carries several problems, such as antiidiotype antibody production, attachment of few cells to the target tissue and limited distribution in both healthy and diseased sites. One of the main reasons for chimeric receptor's failure during clinical trials is the immunogenicity of antibody in the receptor. The antibody usually used in chimeric receptors is ScFv that has a mouse monoclonal antibody origin. Because of the murine origin of ScFv, the antibodies that are produced against it disturb the function of the chimeric receptor. Certainly a great deal of progress has been achieved to humanize these antibodies, but they are still at the immunogenic stage [29, 30].

With respect to VHH properties and solving the immunogenicity of chimeric receptors, this study involved the use of a gene construct containing the VHH fragment. This antibody was raised against MUC1 with suitable properties (Tarbiat Modares University, Iran) [23]. MUC1 is an epithelial membrane mucin, which in its glycosylated form, covers the gastrointestinal epithelium. Most breast cancers and many pancreas, colon, ovary, and prostate adenocarcinomas have increased expression of this antigen showing a change in its O-glycosylation pattern [31, 32].

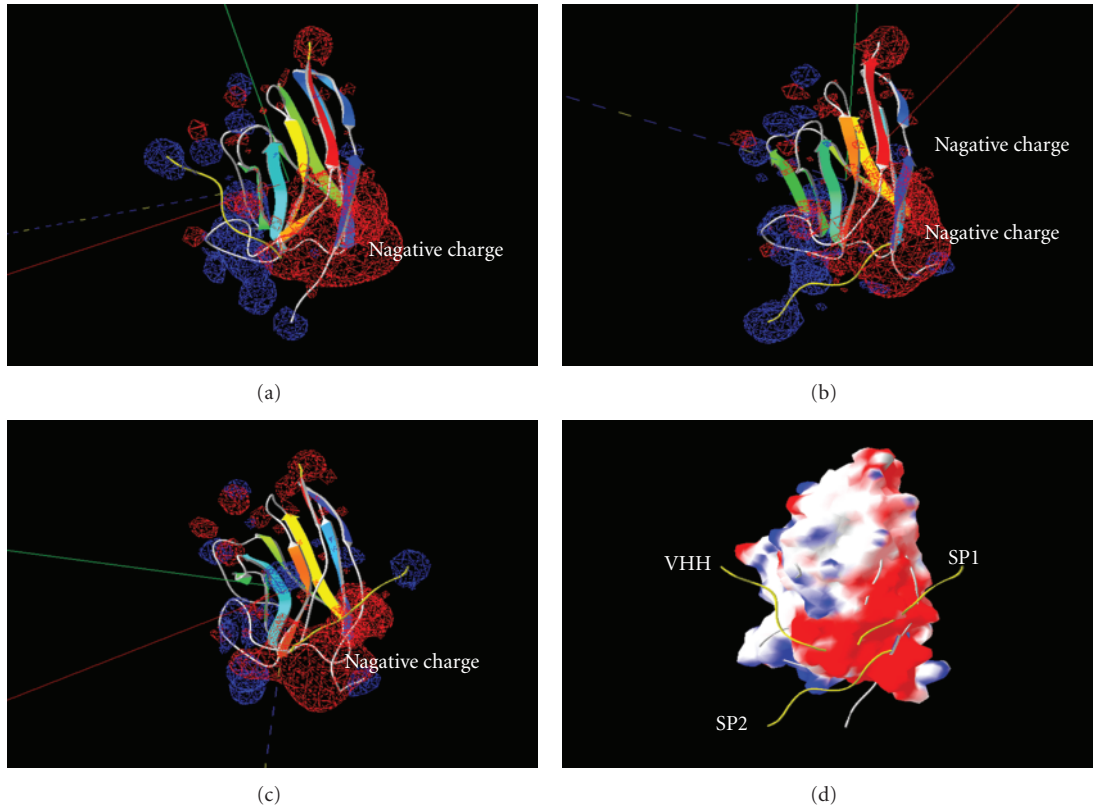

Figure 3: Surface charge distribution of (a) native VHH, (b) VHH plus spacer 1, (c) VHH plus spacer 2 with MUC1 target sequence, and (d) the orientation of the three VHHs (native VHH, VHH plus spacer 1 and VHH plus spacer 2) with MUC1 target sequence, simultaneously.

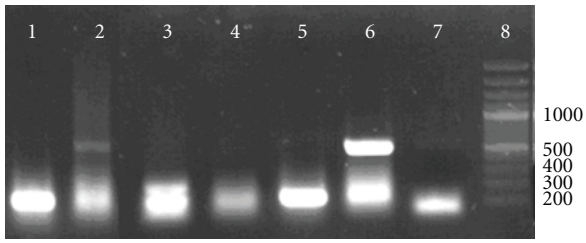

Figure 4: Agarose gel electrophoresis of CD28ζ PCR product. Lane 1: transfected cells with pZCC and β-actin primers. Lane 2: transfected cells with the pZCC and CD28ζ primers. Lane 3: transfected cells with the control vector and β-actin primers. Lane 4: transfected cells with control vector and CD28ζ primers. Lane 5: transfected cells with the pZCF vector and β-actin primers. Lane 6: transfected cells with the pZCF vector and CD28ζ primers. Lane 7: negative control. Lane 8: MW DNA size marker (fermentas).

Such proof and evidence, and high expression in a wide range of MUC1 in cancers, make this molecule a suitable and proper target for chimeric receptor usage [31]. Therefore, based on these findings, this study was divided into two theoretical and experimental phases. In the theoretical study, parameters, such as structural conformational changes, structural fluctuation, and energy of MUC1 interaction with native VHH and VHH carrying each of the spacer sequences were investigated to select the most appropriate spacer sequence. As previously mentioned, the native VHH structure, when compared to VHH carrying each of the CD8α and FcgIIα spacers, showed a deviation of 4.13 Å and 3.67 Å, respectively. These two deviations involving the binding sequences are related to amino acids 4–11 in VHH plus CD8α and VHH plus FcgIIα, respectively. Furthermore, deviations of 5.89 Å and 5.39 Å involving the binding sequence are related to amino acids 105–122 in both VHH plus CD8α and VHH plus FcgIIα. Therefore, it can be concluded that the deviation level in the binding sequence of VHH plus FcgIIα is slightly less, thus indicating a smaller deviation from the native VHH structure, which suggests that the FcgIIα spacer has a lesser effect on the final VHH conformation. This conformational change in the binding region can affect the binding pattern and function of the construct. Another parameter studied was structural fluctuation which, as mentioned before, changes in the presence of each spacer, and the pattern of change differs in the CD8α and FcgIIα spacers.

Structural fluctuations between native VHH and VHH containing the CD8α spacer showed an increase in fluctuation in the amino acid regions 5–13, 29–32, 112–117, and a decrease in the amino acids 58–61 and 105–110. These amino acids correlate with amino acids 5–12, 113–122 at the binding site of VHH carrying the CD8α spacer and the MUC1 target sequence, which shows that fluctuation at the

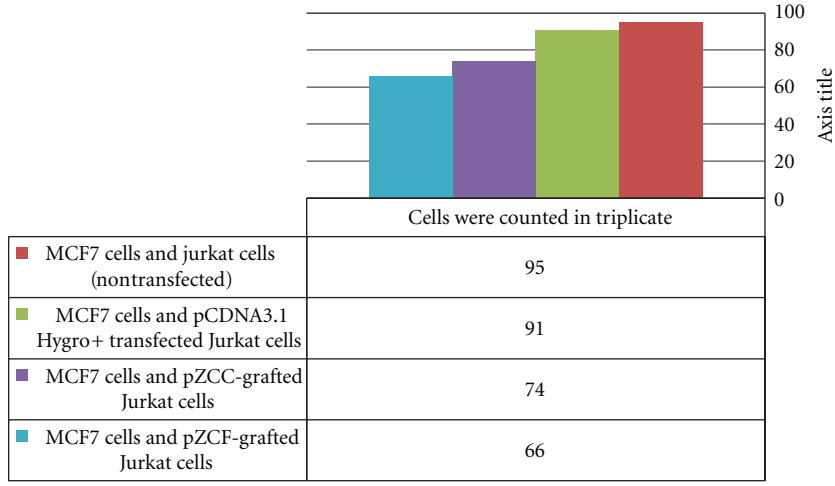

Figure 5: Increase in Jurkat cell numbers in various coculturing conditions after 24 hours incubation.

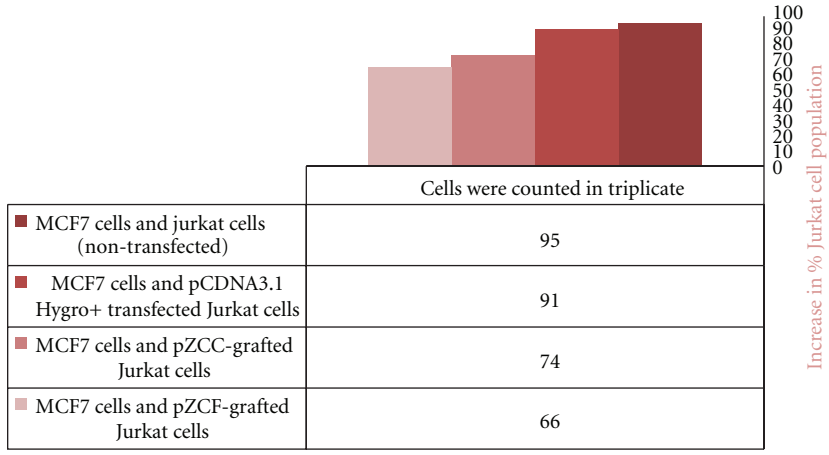

Figure 6: Cytotoxicity of MCF7 cells after 24 hours of incubation.

binding site in the presence of the CD8α spacer demonstrates a significant change. Structural fluctuations between native VHH and VHH containing the FcgIIα spacer also showed an increase in fluctuation in the amino acid regions 30–36 and a decrease in amino acid regions 59–75 and 86–96. These amino acids do not overlap with the region involved in the binding of VHH carrying the FcgIIα spacer and the MUC1 target sequence.

As mentioned in the results, the total energy of interaction regarding the native VHH, VHH plus CD8α spacer, and VHH plus FcgIIα with the MUC1 target sequence was -40.2, -36.0, and -46.9 Kcal/mol, respectively. With respect to the amino acids involved in binding, interactions with the MUC1 target sequence occur at similar binding sites but with different binding energies. Because the binding energy of VHH plus FcgIIα with MUC1 is more negative, binding is stronger and precise due to the conformational changes of VHH in the presence of the FcgIIα spacer. Hence, it can be concluded that the FcgIIα spacer is a more appropriate candidate regarding the CD8α spacer.

Although theoretical studies ascribed the FcgIIα spacer to be more suitable, its extent of effectiveness on signal transduction was assessed by experimental procedures. The fact is that small changes in the affinity and the duration of connection of the receptor to the related ligand can lead to remarkable responses in signal transduction; therefore, the assessment of change in the binding energy generated from the connection of the ligand to the receptors can be very useful in the construction of specific receptors against cancer antigens.

With extensive studies carried out on chimeric receptors and the comparison of results obtained from the studies, the best selections regarding the design of chimeric receptors were made. Consequently, the CD3Zeta fragment and CD28 were selected as signaling domain and costimulating moiety, respectively, and CD8α and FcgIIα were selected as spacers regions. Each spacer sequence was obtained from the NCBI database, and primers were designed accordingly.

Chimeric receptor expression at the mRNA level in the transfected cells relative to β-actin as control was found to be

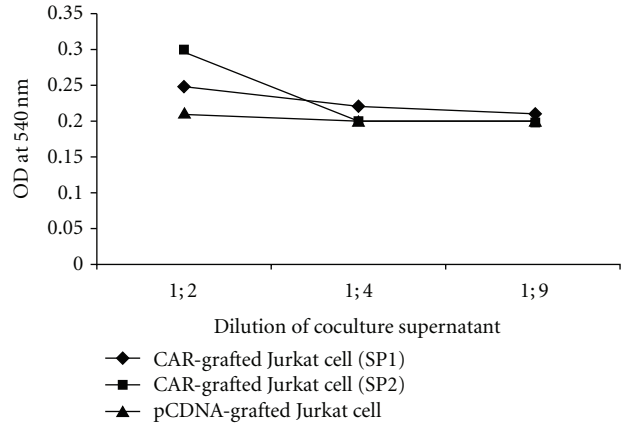

Figure 7: Bioassay results for IL-2 secretion by the two CAR-grafted Jurkat cell lines and pCDNA3.1 Hygro+ transfected Jurkat cells at an optical density (OD) of 540 nm.

very high, with an absence of response in the untransfected cells (control cells) and those transfected with the vector derived from the chimeric receptor (control vector). The results showed desirable expression and good activity regarding the constructed chimeric receptors, thus confirming the previous theoretical studies, which showed high levels of chimeric receptor expression in the cells. Inclusively, the function of the chimeric receptor was assessed using the bioassay test. The proliferation of the two recombinant receptor-grafted Jurkat cells was enhanced upon incubation with MCF7 tumor cells, while vector-transfected Jurkat cells had a significantly lower rate of proliferation. Furthermore, the ability of receptor-grafted Jurkat cells to lyse MCF7 cells was assessed. Receptor-grafted Jurkat cells lysed MCF7 cells with high efficiency, whereas no similar effect was observed when coculturing with the control vector-transfected Jurkat cells. Lysis of MCF7 cells in this experiment indicated that the death of MCF7 cells was receptor dependent, since the control Jurkat cells were unable to significantly induce MCF7 cell lysis. Jurkat cells secrete IL-2 upon stimulation and encountering their target antigen. The proliferation rate of CTLL2 cells in the supernatant of the Jurkat and MCF7 coculture implies that the receptor-grafted Jurkat cells produce more IL-2. Since the proliferation of CTLL2 cells is positively correlated to the IL-2 levels, the data indicate that receptor-grafted Jurkat cells produce more IL-2 in comparison with the control vector-transfected Jurkat cells.

The results of theoretical studies indicated that the total energies of interaction of native VHH, VHH plus CD8α spacer, and VHH plus FcgIIα with the MUC1 target sequence were -40.2, -36.0, and -46.9 Kcal/mol, respectively. So, the more negative binding energy of VHH plus FcgIIα with MUC1suggests a much stronger binding. It is predicted that the effect of an increase in the interaction can more suitably affect the transduction of signals into the cell for the purpose of IL2 production.

5. Conclusions

In fact, the results from the experimental phase support these assumptions and predictions derived from the theoretical study. However, the striking point is to what extent does a -10.9 Kcal/mol difference affect the function and effectiveness of chTCR. Experimental results showed that this slight difference in the interaction energy caused a significant increase in receptor effectiveness (the signal transduction process and IL2). Therefore, prior to any functional sequence selection in a chimeric receptor cassette, as in the case of this study, it is necessary to investigate the simulation stability, structural fluctuation, interaction simulation and finally the charge distribution in the peptide receptor domain, and the ligand of interest as parameters in theoretical studies.

Nevertheless, the theoretical and experimental results of this study show that despite a larger spacer size causing better exposure of the antibody for penetration and accessibility to membrane antigens in cancer cells (especially antigens with MUC1 structural properties), the better exposure of chTCR cannot be the only reason for the increase in antibody function regarding interaction with the antigen. In fact, the better interaction is the consequence of the peptide sequence effect in the chimeric receptor and enhanced antibody exposure. With consideration of these results and VHH's unique properties, it is hoped that the functional problems of chimeric receptors can be solved. In order to expand on the above findings, it is better to continue the research by considering the following items: (a) substitution of signaling, spacer, and costimulating fragments with other fragments from other studies and investigation of their functions; (b) substitution of VHH against MUC1 with VHH raised against other cancer antigens and investigation of their functions; (c) carrying out mutagenesis of VHH and investigating the effects of mutations on structural properties and activities which increase the extent of chTCR binding.

Acknowledgments

The authors thank Mrs. Parvin Shariati for her help with editing the paper. The authors also express their gratitude to the research council of the University of Guilan and Ministry of Sciences, Researches, and Technology for financial support during the course of this project.

References

[1] C. H. June, "Principles of adoptive T cell cancer therapy," *Journal of Clinical Investigation*, vol. 117, no. 5, pp. 1204–1212, 2007.

[2] C. Yee, "Adoptive T-Cell Therapy of Cancer," *Hematology/Oncology Clinics of North America*, vol. 20, no. 3, pp. 711–733, 2006.

[3] S. K. Tey, C. M. Bollard, and H. E. Heslop, "Adoptive T-cell transfer in cancer immunotherapy," *Immunology and Cell Biology*, vol. 84, no. 3, pp. 281–289, 2006.

[4] M. Barry and R. C. Bleackley, "Cytotoxic T lymphocytes: all roads lead to death," *Nature Reviews Immunology*, vol. 2, no. 6, pp. 401–409, 2002.

[5] W. Y. Ho, C. Yee, and P. D. Greenberg, "Adoptive therapy with CD8+ T cells: it may get by with a little help from its friends," *Journal of Clinical Investigation*, vol. 110, no. 10, pp. 1415–1417, 2002.

[6] C. H. June, "Adoptive T cell therapy for cancer in the clinic," *Journal of Clinical Investigation*, vol. 117, no. 6, pp. 1466–1476, 2007.

[7] A. Murphy, J. A. Westwood, L. E. Brown et al., "Antitumor activity of dual-specific T cells and influenza virus," *Cancer Gene Therapy*, vol. 14, no. 5, pp. 499–508, 2007.

[8] Z. Eshhar, "The T-body approach: redirecting T cells with antibody specificity," *Handbook of experimental pharmacology*, no. 181, pp. 329–342, 2008.

[9] A. Hombach, A. Wieczarkowiecz, T. Marquardt et al., "Tumor-specific T cell activation by recombinant immunoreceptors: CD3 zeta signaling and CD28 costimulation are simultaneously required for efficient IL-2 secretion and can be integrated into one combined CD28/CD3 zeta signaling receptor molecule," *Journal of Immunology*, vol. 167, no. 11, pp. 6123–6131, 2001.

[10] K. Kronfeld, E. Hochleitner, S. Mendler et al., "B7/CD28 costimulation of T cells induces a distinct proteome pattern," *Molecular and Cellular Proteomics*, vol. 4, no. 12, pp. 1876–1887, 2005.

[11] M. Karplus, "Dynamics of proteins," *Advances in Biophysics*, vol. 18, pp. 165–190, 1984.

[12] M. Karplus and J. A. McCammon, "The dynamics of proteins," *Scientific American*, vol. 254, no. 4, pp. 42–51, 1986.

[13] M. Karplus, S. Swaminathan, T. Ichiye, and W. F. Van Gunsteren, "Local and collective motions in protein dynamics," *Ciba Foundation Symposium*, vol. 93, pp. 271–290, 1983.

[14] W. R. Cannon, S. F. Singleton, and S. J. Benkovic, "A perspective on biological catalysis," *Nature Structural Biology*, vol. 3, no. 10, pp. 821–833, 1996.

[15] R. J. P. Williams, "Are enzymes mechanical devices?" *Trends in Biochemical Sciences*, vol. 18, no. 4, pp. 115–117, 1993.

[16] T. A. Sulchek, R. W. Friddle, K. Langry et al., "Dynamic force spectroscopy of parallel individual Mucin1-antibody bonds," *Proceedings of the National Academy of Sciences of the United States of America*, vol. 102, no. 46, pp. 16638–16643, 2005.

[17] D. M. Webster, *Protein Structure Prediction: Methods and Protocols (Methods in Molecular Biology)*, vol. 143, Humana Press, Totowa, NJ, USA, 2000.

[18] D. A. Case, T. A. Darden, T. E. Cheatham III et al., *AMBER: Version 9*, University of California, San Francisco, Calif, USA, 2004.

[19] Y. Duan, C. Wu, S. Chowdhury et al., "A point-charge force field for molecular mechanics simulations of proteins based on condensed-phase quantum mechanical calculations," *Journal of Computational Chemistry*, vol. 24, no. 16, pp. 1999–2012, 2003.

[20] T. Darden, D. York, and L. Pedersen, "Particle mesh Ewald: an N·log(N) method for Ewald sums in large systems," *The Journal of Chemical Physics*, vol. 98, no. 12, pp. 10089–10092, 1993.

[21] W. L. Jorgensen, J. Chandrasekhar, J. D. Madura, R. W. Impey, and M. L. Klein, "Comparison of simple potential functions for simulating liquid water," *The Journal of Chemical Physics*, vol. 79, no. 2, pp. 926–935, 1983.

[22] P. Aloy, G. Moont, H. A. Gabb, E. Querol, F. X. Aviles, and M. J. E. Sternberg, "Modelling repressor proteins docking to DNA," *Proteins*, vol. 33, no. 4, pp. 535–549, 1998.

[23] S. H. A. Bakhtiari, F. Rahbarizadeh, S. Hasannia, D. Ahmadvand, F. J. Iri-Sofla, and M. J. Rasaee, "Anti-MUC1 nanobody can redirect T-body cytotoxic effector function," *Hybridoma*, vol. 28, no. 2, pp. 85–92, 2009.

[24] S. Xue, R. Gillmore, A. Downs et al., "Exploiting T cell receptor genes for cancer immunotherapy," *Clinical and Experimental Immunology*, vol. 139, no. 2, pp. 167–172, 2005.

[25] M. Coccoris, M. A. de Witte, and T. N. M. Schumacher, "Prospects and limitations of T cell receptor gene therapy," *Current Gene Therapy*, vol. 5, no. 6, pp. 583–593, 2005.

[26] Z. Eshhar, "The T-body approach: redirecting T cells with antibody specificity," *Handbook of Experimental Pharmacology*, no. 181, pp. 329–342, 2008.

[27] A. Hombach and H. Abken, "Costimulation tunes tumor-specific activation of redirected T cells in adoptive immunotherapy," *Cancer Immunology, Immunotherapy*, vol. 56, no. 5, pp. 731–737, 2007.

[28] K. Kronfeld, E. Hochleitner, S. Mendler et al., "B7/CD28 costimulation of T cells induces a distinct proteome pattern," *Molecular and Cellular Proteomics*, vol. 4, no. 12, pp. 1876–1887, 2005.

[29] A. Murphy, J. A. Westwood, L. E. Brown et al., "Antitumor activity of dual-specific T cells and influenza virus," *Cancer Gene Therapy*, vol. 14, no. 5, pp. 499–508, 2007.

[30] F. Thistlethwaite, W. Mansoor, D. E. Gilham, and R. E. Hawkins, "Engineering T-cells with antibody-based chimeric receptors for effective cancer therapy," *Current Opinion in Molecular Therapeutics*, vol. 7, no. 1, pp. 48–55, 2005.

[31] T. A. Sulchek, R. W. Friddle, K. Langry et al., "Dynamic force spectroscopy of parallel individual Mucin1-antibody bonds," *Proceedings of the National Academy of Sciences of the United States of America*, vol. 102, no. 46, pp. 16638–16643, 2005.

[32] Y. Li and P. J. Cozzi, "MUC1 is a promising therapeutic target for prostate cancer therapy," *Current Cancer Drug Targets*, vol. 7, no. 3, pp. 259–271, 2007.